T-shaped quantum wires in magnetic fields: Weakly confined magnetoexcitons beyond the diamagnetic limit

Garnett W. Bryant[1,*] and Y. B. Band[1,2,†]
[1]*National Institute of Standards and Technology, 100 Bureau Drive, Stop 8423, Gaithersburg, Maryland 20899*
[2]*Departments of Chemistry and Physics, Ben-Gurion University of the Negev, Beer-Sheva, 84105 Israel*
(Received 18 August 2000; revised manuscript received 4 December 2000; published 22 February 2001)

Optical excitations of magnetoexcitons in T-shaped wires are calculated and compared with experiment. We find the single-particle states for electrons and holes confined to a wire in a magnetic field and use these states as a basis for calculations of magnetoexciton states. We accurately reproduce the field dependence of the exciton states and explain the small, field-induced, energy shifts that are observed for these states. The shifts are small because the T-junction provides weak confinement, rather than strong quantum confinement. Diamagnetic shifts calculated from perturbation theory fail to describe the experimental results. We determine when perturbation theory is valid for these nanostructures and which gauge should be used to give the diamagnetic shift that best reproduces the field dependence at low fields.

DOI: 10.1103/PhysRevB.63.115304 PACS number(s): 73.21.−b, 85.35.Be, 78.66.−w, 71.35.Ji

I. INTRODUCTION

The development of semiconductor quantum wires and dots has progressed rapidly in recent years. Quantum wire nanostructures can be fabricated now with monolayer precision, with dimensions of a few nanometers, free from damage due to lithographic processing, and in high density by the use of all-growth fabrication processes based on epitaxial techniques. One of the most successful all-growth techniques for fabricating wires has been cleaved edge overgrowth.[1–25] In this approach, T-shaped wires are created at the intersections between orthogonal quantum wells with the wire axis perpendicular to the cross section shown in Fig. 1. For GaAs/AlGaAs wires, these intersections are made by growing a [110] GaAs quantum well (the arm well) on the cleaved edge of a multiple [100] GaAs/AlGaAs quantum well system (the stem wells). Electrons and holes are trapped at the T-shaped intersections because the single-particle confinement energy is lower in the intersections of the stem and arm wells than in either the stem or arm wells.[1]

In this paper we present the first calculation of confined magnetoexciton states and energies in T-shaped wires. We use an extension of the theory developed to calculate exciton states at vanishing magnetic field[26] to $B \neq 0$. Exciton states for interacting electron-hole pairs confined to a T-shaped intersection in a finite magnetic field are calculated by determining exactly the single-particle states confined to the T intersection in a magnetic field and then using these single-particle states as a basis for a configuration-interaction calculation to include the pair interaction. We then compare our results for magnetoexciton energies with experiments[9] and with the previous interpretation of these experiments.[9]

A wire nanostructure is considered to be in the one-dimensional (1D) quantum limit when the electron-hole interaction can modify the electron-hole pair relative motion along the wire axis (z axis in Fig. 1) but is not strong enough to mix the single-particle lateral sublevels. In a 1D quantum wire, the interacting electron and hole occupy individual single-particle lateral sublevels. In simple models for excitons in ideal wires, lateral confinement is usually defined by a high-barrier (hard wall) potential. In this case, the electron and hole have similar lateral wave functions that are determined by the geometry of the confinement and are not sensitive to the particle masses. The 1D, strong-confinement limit is approached by reducing the lateral dimension of the wire. Such a simple model cannot be used to describe excitons in T-shaped wires.[26] In T-shaped wires, the confinement to the wire region is determined both by the geometry of the barriers that define the structure and by the differences between the confinement energy in the T-shaped intersection region and confinement energies in the arm and stem wells. Because the energy differences are small, the confinement is weak, i.e., quasi-1D, and electron-hole correlation in the lateral directions, as well as along the wire axis, must be included.[26] In simple models for quantum wires, one geometrical parameter, such as the wire radius, defines the size scale for the confinement. In simple wires, the particles are squeezed inside the wire as the confinement increases. In T-shaped wires, the confinement is a complicated competition between confinement along the stem and arm wells. The confinement is squishy. When the confinement along one well is increased, either by decreasing the well width or by allowing more pair correlation in that direction, confinement along the orthogonal well can decrease, i.e., squeezing the exciton in one well pushes the exciton out of the wire into the other well.[26]

To understand the effects of this squishy confinement on the electron and hole confinement energies and on the exciton binding energies, exciton states in these structures must be characterized fully. T-shaped wires have been characterized extensively by photoluminescence (PL) spectroscopies.[1–25] Typical exciton PL spectra exhibit peaks due to PL from the stem and arm wells and from the wires. Spatially resolved PL[4,8,14,18] has been measured to separate the wire PL from stem and arm well PL. The lowest-energy PL peak is due to excitons trapped in the wires. Redshifts between the wire and well PL as large as 34–54 meV have been observed.[7,10,17,24] This redshift is due partly to the reduction in single-particle confinement energy when the elec-

trons and holes are trapped at the T-shaped intersections and partly to the enhancement of the electron-hole binding energy when the exciton is trapped in a wire. Binding energies as large as 26 meV (six times the bulk binding energy) have been estimated.[12] These large redshifts strongly suggest that the excitons have been trapped into 1D wire states. Measurements of the optical polarization anisotropy[13,14] provide additional evidence for the crossover from 2D to 1D states upon confinement of the exciton into the wires.

Exciton PL peak energies and transition strengths give information about excitonic confinement in T-shaped wires that depends on the combined effects of the squishy lateral confinement and the enhanced binding. To fully assess the degree of 1D quantization and better separate confinement and binding effects, complementary information about the spatial extent of the exciton wave functions is required. Recently, Someya, Akiyama, and Sakaki[9,16,20] studied the magnetophotoluminescence of T-shaped wires. They measured the energy shift ΔE of PL peaks with magnetic field B applied perpendicular to the wire axis and parallel to the stem well (as shown in Fig. 1). They related the measured energy shift ΔE to a quadratic shift, $\Delta E=\beta B^2$, and extracted the lateral size of the exciton by assuming that β was the diamagnetic coefficient appropriate for excitons which are symmetric about the magnetic field axis ($\beta=e^2r^2/8\mu$ where μ and $r=\sqrt{\langle x^2+z^2\rangle}$ are the exciton reduced mass and radius perpendicular to B). They analyzed wires made with large wells (wire S_1: $a=10$ nm, $b=12.5$ nm and wire S_2: $a=5.8$ nm, $b=6.8$ nm) and wires made with smaller wells (wire S_3: $a=5.1$ nm, $b=5.6$ nm and wire S_4: $a=5.1$ nm, $b=5.1$ nm). Excitons trapped at the T intersections have much smaller field-induced energy shifts than the excitons in the arm well. The weaker response of the trapped exciton to the applied magnetic field suggests that the the trapped exciton has a smaller lateral size than the exciton in the arm well. The extracted values of r for the wire excitons in wires S_3 and S_4 are smaller than the lateral size of an exciton in an ideal, strictly 2D quantum well. The analysis of Someya, Akiyama and Sakaki suggests that excitons in T-shaped wires can be squeezed below the minimum size realized by 2D excitons in GaAs quantum wells. In this limit, the wires must be 1D quantum wires.

Previously, we developed a theory for excitons in T-shaped quantum wires at zero magnetic field.[26] The theory used an anisotropic effective-mass model for the electrons and holes. Electron and hole single-particle states trapped at the T-shaped intersections were found exactly. The electron-hole pair binding in the exciton state was determined through a configuration interaction approach. A good description of exciton ground states was obtained. We found that including lateral electron-hole correlation as well as correlation along the wire axis was necessary to describe zero-field PL shifts observed for wire excitons.[3,9] For the wires that we modeled, lateral wave function mixing was important. The wires could not be treated as strictly 1D. We also calculated the lateral size of the exciton state from the calculated exciton wave function.[26] The calculated lateral sizes were much larger than the sizes extracted from the analysis of the magneto PL experiments.[9]

This discrepancy between theory and analysis of the experimental data could be explained in two ways. Either the zero-field theory provides a description of the exciton size that is not as good as suggested by the good description of the zero-field confinement-induced PL redshifts, or the analysis of the experimental data is not adequate. The experimental data was taken for magnetic fields up to 12 T. However, the analysis of the data was done assuming a weak field limit, where perturbation theory for the magnetic-field induced energy shifts ΔE determines the diamagnetic contribution to the quadratic energy shift of the PL peak. The only contribution to the quadratic energy shift included in the analysis was the diamagnetic contribution. The second-order contribution that arises from the paramagnetic van Vleck contribution, that is important when the exciton is not symmetric about the magnetic field axis, was not included.

To better understand excitons in T-shaped wires, we provide in this paper a detailed theory for these magnetoluminescence experiments. To develop a theory for magnetoexcitons in T-shaped wires, we extend the model that we used for zero-field excitons to finite magnetic field. We find the single-particle states exactly, now at finite field, and we include the electron-hole binding in a configuration interaction approach. This allows us to find exactly (for our model) the trapped exciton states at each magnetic field and to calculate the exciton energy shifts with applied magnetic field without recourse to perturbation theory.

This paper is organized as follows. In Sec. II, we describe briefly the theory that we previously used for the zero-field case and discuss the results that show that three-dimensional (3D) correlation is needed to describe excitons in T-shaped wires. We then present the extension of the theory to finite magnetic field. A key feature for any theory at finite field is the choice of gauge used to describe the magnetic field. In an exact calculation for the magnetic field effects, the results cannot depend on the choice of gauge. In perturbation theory, the choice of gauge can be important if the perturbation theory is not done completely. We show why perturbation theory based on the diamagnetic contribution fails for T-shaped wires. In Sec. III, we present our results. We first discuss exact calculations for single-particle states of the T-shaped wire in a magnetic field. We also provide an exact calculation from perturbation theory of the second order contribution to the single-particle energies. We show that perturbation theory, even if done correctly, fails for $B>2$ T. We present results for the field dependence of the single-particle wave functions to show that perturbation theory fails because the confinement provided by the T-shaped junctions is squishy. We then present results for excitons in T-shaped wires in a magnetic field. We show that we get good agreement with experiment when we go beyond perturbation theory and include magnetic field effects exactly in our model. In Sec. IV, we present our conclusions.

II. THEORY

Various theories have been presented for zero-field exciton states in T-shaped wires.[21,26–33] Typically, the single-particle electron and hole states trapped at a T-shaped inter-

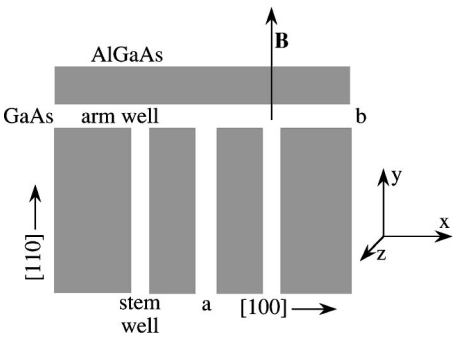

FIG. 1. Cross sectional view of an array of T-shaped wires. *a* is the width of the [100] stem wells and *b* is the width of the [110] arm well. The direction of the applied magnetic field *B* used for magnetophotoluminescence is shown.

section are found by use of a single- or multi-band effective-mass model and the Coulomb effects are included either variationally, in the Hartree-Fock approximation, or in a multiconfigurational approach. Our calculation for magnetoexcitons in T-shaped wires is based on an extension of the theory that we used to calculate exciton states at $B=0$ to finite field.[26] We calculate exciton states for interacting, electron-hole pairs confined to a T-shaped intersection in a finite magnetic field by first determining exactly the single-particle states confined to the T-intersection in a magnetic field and then using these single-particle states as a basis for a configuration-interaction calculation to include the pair interaction. In the next section we briefly review the calculation of exciton states at $B=0$.

A. Exciton states at $B=0$

Our calculation proceeds in two step.[26] First, we find the electron and hole single-particle states bound to a finite array of T-shaped wires, as shown in Fig. 1. We use an isotopic single-band, effective-mass Hamiltonian for the electron single-particle states. To find hole single-particle states, we use an anisotropic, single-band, effective-mass Hamiltonian. We ignore the effects of band-mass discontinuity at the well/barrier interfaces and use the well masses throughout the structure. For these single-particle Hamiltonians, motion along the wire axis, the *z* direction, is separable from the lateral motion, the *x* and *y* directions. We find the bound, lateral, electron and hole states ϕ_n^e and ϕ_n^h with energies E_n^e and E_n^h by solving,

$$H_{2D}^e\phi_n^e=\left[-\frac{\hbar^2}{2m_e}\left(\frac{\partial^2}{\partial x^2}+\frac{\partial^2}{\partial y^2}\right)+V_{2D}^e\right]\phi_n^e=E_n^e\phi_n^e, \tag{1}$$

$$H_{2D}^h\phi_n^h=\left(-\frac{\hbar^2}{2m_{hx}}\frac{\partial^2}{\partial x^2}-\frac{\hbar^2}{2m_{hy}}\frac{\partial^2}{\partial y^2}+V_{2D}^h\right)\phi_n^h=E_n^h\phi_n^h.$$

V_{2D}^e and V_{2D}^h are the two-dimensional T-shaped potentials defined by the GaAs/AlGaAs band offsets, m_e is the isotropic, conduction-band mass in GaAs and m_{hi} is the hole mass for direction *i*. Fourier grid techniques are used to find the bound states. The grid covers the area occupied by the states bound to the wire array. Typically, an array with *N* wires has *N* bound states.

These bound single-particle states are used to define electron-hole pair states for configuration-interaction calculations to account for the pair binding. We find the exciton ground state by solving,

$$H_{3D}^{ex}\Psi^{ex}=\left(H_{2D}^e+H_{2D}^h-\frac{\hbar^2}{2\mu_z}\frac{\partial^2}{\partial z^2}+V_{3D}^{eh}\right)\Psi^{ex}=E^{ex}\Psi^{ex}, \tag{2}$$

where $z=z_e-z_h$ and $1/\mu_z=1/m_e+1/m_{hz}$ are the pair relative-coordinate and reduced mass along the wire axis. V_{3D}^{eh} is the static, screened Coulomb interaction,

$$V_{3D}^{eh}(\mathbf{x}_e,\mathbf{x}_h)=\frac{q_eq_h}{\epsilon\sqrt{(x_e-x_h)^2+(y_e-y_h)^2+z^2}}, \tag{3}$$

where q_e and q_h are the electron and hole charge and ϵ is the dielectric constant. We expand the exciton wave function Ψ^{ex} as

$$\Psi^{ex}(\mathbf{x}_e,\mathbf{x}_h)=\sum_{n,m,\eta_x,\eta_y,\eta_z}\alpha_{n,m,\eta_x,\eta_y,\eta_z}\phi_n^e(\mathbf{x}_e)\times\phi_m^h(\mathbf{x}_h)\chi_{\eta_x,\eta_y,\eta_z}(\mathbf{x}_e,\mathbf{x}_h), \tag{4}$$

where the sum extends over the two-dimensional (2D) lateral states bound to the wire array and $\chi_{\eta_x,\eta_y,\eta_z}$ accounts for any pair correlation in each direction

$$\chi_{\eta_x,\eta_y,\eta_z}(\mathbf{x}_e,\mathbf{x}_h)=\exp[-\eta_x(x_e-x_h)^2-\eta_y(y_e-y_h)^2-\eta_zz^2]. \tag{5}$$

We diagonalize the Hamiltonian in this basis to find the lowest exciton state and vary the η_i included in the sum to minimize the ground state energy. We include a sufficient number of η's to obtain the 3D limit in large structures and to correctly model both wells and wires. We use the same theory to describe exciton states in wires and in wells so that we can determined the energy difference between these states to compare with the measured redshifts between well and wire PL peaks. The η_z determine the correlation along the wire axis. The η_x and η_y determine any lateral correlation that is not included in the sum over lateral states. To study excitons in a single wire, the sum over *n* and *m* is over the electron states and hole states bound to the wire. In all cases that we have studied, a single wire has only one bound electron state and one bound hole state. When there is only one bound electron or hole state, no lateral correlation is included in the sum over bound lateral states. The lateral correlation comes from mixing unbound lateral states with the bound state. This mixing is accounted for in our calculation by the sum of lateral correlation factors over η_x and η_y. When we set $\eta_x=\eta_y=0$, we include correlation only along the wire axis, as would be appropriate for an ideal 1D quantum wire.

TABLE I. Experimental[9] and calculated exciton redshifts ΔE at zero field for wires S_1-S_4. Experimental quadratic coefficient $\beta_{\rm exp}$[9] and the calculated diamagnetic coefficient β^L.

Wire	$\Delta E_{\rm exp}$ (meV)	$\beta_{\rm exp}$ (μeV/T^2)	Calculation	$\Delta E_{\rm calc}$	β^L
S_1	6	31	isotropic hole, 3D correlation	4.0	57
S_2	11	23	isotropic hole, 3D correlation	10.8	37
S_3	13	18	anisotropic hole, 3D correlation	11.8	77
S_4	16	13	anisotropic hole, 3D correlation	16.2	69

To model GaAs/AlGaAs structures, we use $\epsilon=13.1, m_e=0.067$ and a conduction band/valence band offset ratio of 62:38.[34] Other similar choices for ϵ to model polarization effects and for m_e to model band parabolicity give similar results for the exciton redshifts provided that the same model is used to find the exciton states in both wells and wires. We consider two models for the hole states. In the simpler model, we assume that the hole has an isotropic, heavy mass, $m_h=0.33$. This model should work best for structures made from larger wells, such as S_1 and S_2, where confinement effects are weaker and the splitting of hole states by the confinement is less important than the mixing of states by the Coulomb interaction. We also consider a model with an anisotropic hole-mass, appropriate for a hole in the [110] arm well, with $m_{hx}=m_{hz}=0.13$ and $m_{hy}=0.34$. This model should be most appropriate for structures made from small wells, such as S_3 and S_4, where the strong arm-well confinement splits the degenerate hole-states into heavy and light holes.

We find that the PL peak energy shift is well described in wires S_1 and S_2 by the model with the isotropic hole-mass and in wires S_3 and S_4 by the model with the anisotropic hole-mass. Results are listed in Table I. This is consistent with our expectation that the isotropic model should work better for larger structures and the anisotropic model should work better for smaller structures. We find the exciton must be modeled as a 3D exciton even though it is confined to the wire. Correlation must be included in all three dimensions to get a good description of the exciton energy shifts. Including only 1D correlation along the wire axis does not provide the enhanced pair binding when the exciton is trapped in the wire. For S_3 and S_4, the calculated binding provided by 1D correlation is even weaker that the calculated binding for the exciton in the arm well. These results are described in detail in Ref. 26.

From the exciton ground state wave function, we calculate the lateral spread of the exciton state $r=\sqrt{\langle (x_e-x_h)^2+z^2\rangle}$ and the diamagnetic contribution, found in the symmetric gauge by perturbation theory (see the next section), for the quadratic shift of the exciton energy with applied magnetic field, $\beta^L=e^2r^2/8\mu$. A comparison of the experimental quadratic coefficient and the diamagnetic coefficient calculated at zero field is given in Table I. The energy shifts at $B=0$ are well described by the theory. However, perturbation theory gives a poor description of the quadratic coefficient. The r extracted from experimental β^L for S_3 and S_4 fall below the lower limit for the size of an exciton confined to an ideal 2D well.[9] This suggests that S_3 and S_4 are small enough to be 1D *quantum* wires. The calculated r are significantly higher than the experimental r and are above the 2D limit for each wire. As we will show, the field dependence of the exciton states can be described if the field dependence is determined exactly. We will also show that perturbation theory fails to describe the field dependence of the exciton energies and cannot be used to extract r from the experimental data. In the next section we describe the extension of our $B=0$ theory to include a magnetic field.

B. Magnetoexcitons

To study magnetoexcitons, we extend the zero-field model defined by Eqs. (1)–(5) to include a magnetic field. The kinetic energy operator is

$$T_{3D}^{e,h}=T_{3D}^{e}+T_{3D}^{h}=\frac{\left(\mathbf{p}_e-\frac{q_e}{c}\mathbf{A}(\mathbf{x}_e)\right)^2}{2m_e}+\sum_i\left(\mathbf{p}_h-\frac{q_h}{c}\mathbf{A}(\mathbf{x}_h)\right)_i\times\frac{1}{m_{h,i}}\left(\mathbf{p}_h-\frac{q_h}{c}\mathbf{A}(\mathbf{x}_h)\right)_i. \tag{6}$$

The total electron-hole Hamiltonian is

$$H^B=T_{3D}^{e}+T_{3D}^{h}+V_{2D}^{e}+V_{2D}^{h}+V_{3D}^{eh}. \tag{7}$$

To proceed further, we must choose a gauge for the vector potential. In principle, the results must be gauge invariant. Any gauge should be appropriate to use. In practice, the choice of gauge is important. Exact calculations can be simplified by a choice of gauge which is consistent with the symmetry of the problem, in our case, the 1D translational symmetry of the wire. A perturbative calculation to second order in B is necessarily gauge invariant only if all second-order contributions are determined exactly. Again, the symmetry of the problem determines which gauge to use to calculate all of the second-order contributions or which gauge to use for the most accurate approximate calculation of these contributions.[35,36]

The symmetric gauge,

$$\mathbf{A^L}(\mathbf{x})=\tfrac{1}{2}\,\mathbf{B}\times\mathbf{x} \tag{8}$$

is often used. In this gauge, the electron kinetic energy for $\mathbf{B}=B\hat{y}$ is

$$T_{3D}^{L,e}=\frac{[\mathbf{p}_e-q_e\mathbf{A}^{\mathbf{L}}(\mathbf{x}_e)/c]^2}{2m_e}$$

$$=\frac{\mathbf{p}_e^2}{2m_e}-\frac{q_eBL_y}{m_ec}+\frac{q_e^2B^2(x_e^2+z_e^2)}{8m_ec^2}. \quad (9)$$

Here L_y is the yth component of the angular momentum operator. The hole kinetic energy is similar. This gauge is useful for studying interacting particles where the imposed symmetry, for example due to confinement, does not break cylindrical symmetry about the field axis. In this case, the states are eigenstates of L_y. Typically the ground state has $L_y=0$ and the only second-order contribution to the energy is the diamagnetic term. For an electron, the diamagnetic contribution in the symmetric gauge is

$$\beta^L B^2=\frac{q_e^2B^2\langle x_e^2+z_e^2\rangle}{8m_ec^2}. \quad (10)$$

The expectation value for the lateral size of the electron ground-state determines the diamagnetic coefficient. Similar expressions apply for the hole and the exciton.

For a T-shaped wire with B applied perpendicular to the wire axis, translational symmetry along the wire axis is inconsistent with the cylindrical symmetry about the field axis that is needed to simplify calculations done in the symmetric gauge. Nonetheless, the diamagnetic contribution in the symmetric gauge has been used to interpret the experimental data.[9] Thus, it is important to know how well this approximation describes magnetic field effects in T-shaped wires.

In the symmetric gauge, the single-particle Hamiltonian for a T-shaped wire is not separable into lateral and axial coordinates and each single-particle eigenstate must be found as a 3D state rather than as the product of a 2D lateral state and a 1D axial state. In a T-shaped wire, the single-particle states are not eigenstates of L_y. Perturbation theory is gauge invariant if the perturbation theory is done exactly. In the symmetric gauge, the first order contribution is proportional to $\langle L_y\rangle$ and typically is zero for the ground state. There are two contributions in second order, the positive diamagnetic term given by Eq. (10) and the paramagnetic Van Vleck contribution. The paramagnetic contribution for an electron in state i is,

$$\beta_{i,para}^L B^2=\sum_{j\neq i}\frac{\left|\left\langle i\left|\frac{q_eBL_y}{m_ec}\right|j\right\rangle\right|^2}{E_{0i}-E_{0j}}, \quad (11)$$

where E_{0j} is the zero-field energy of state j. A similar expression holds for the hole. The paramagnetic contribution vanishes if the state i is an eigenstate of L_y with $L_y=0$. The single-particle wire states are not eigenstates of L_y and the paramagnetic contribution is finite. For a ground state, the paramagnetic contribution is negative, giving a total second-order contribution which is less than the diamagnetic term. Consequently, a determination of the exciton size by relating a measured quadratic shift to the diamagnetic contribution will underestimate the exciton size.

A more useful gauge for studying T-shaped wires with $\mathbf{B}=B\hat{y}$ is a gauge which preserves translational symmetry along the wire axis,

$$\mathbf{A}^{\mathbf{p}}(\mathbf{x})=-Bx\hat{z}. \quad (12)$$

In this gauge, the electron kinetic energy is

$$T_{3D}^{p,e}=\frac{[\mathbf{p}_e-q_e\mathbf{A}^{\mathbf{p}}(\mathbf{x}_e)/c]^2}{2m_e}$$

$$=\frac{\mathbf{p}_e^2}{2m_e}-\frac{q_eBx_ep_z}{m_ec}+\frac{q_e^2B^2x_e^2}{2m_ec^2}. \quad (13)$$

The hole kinetic energy is similar. In this gauge, the single-particle electron and hole Hamiltonians are separable into lateral, (x,y), and axial, z, coordinates since the single-particle states are eigenstates of p_z. The quadratic contribution to the ground-state ($p_z=0$) single-particle energies for the electron and hole can be found exactly from the diamagnetic contribution in this gauge. For the electron,

$$\beta^p B^2=\frac{q_e^2B^2\langle x_e^2\rangle}{2m_ec^2}. \quad (14)$$

This exact expression for the quadratic contribution is different from the diamagnetic contribution given by β^L in the symmetric gauge [Eq. (10)]. β^p is proportional to the expectation value of $x^2/2$, while β^L is proportional to the expectation value of $(x^2+z^2)/8$.

To find magnetoexciton states in T-shaped wires, we proceed as we did before in finding the zero-field states. We first find the electron single-particle 2D lateral states by use of the separable Hamiltonian given by Eq. (13). We use a similar equation to find the hole states. These 2D states are found on the same 2D grid used for the zero-field states. The 2D states depend on p_z. We could define exciton states by mixing single-particle states with different p_z. Instead, we define the exciton states in terms of the 2D, lateral, single-particle, $p_z=0$ states by use of Eqs. (4) and (5). The mixing of other single-particle states with $p_z\neq 0$ into the exciton state is included by the use of the exponential correlation factors. We diagonalize the Hamiltonian for the interacting electron-hole pair in this basis to determine the magnetoexciton states.

III. RESULTS

Two issues are addressed to analyze the magnetophotoluminescence of T-shaped wires. First, we determine the magnetic-field dependence of single-particle energies in T-shaped wires. We compare the exact single-particle energies with the exact quadratic contribution obtained from β^p to determine the accuracy of the quadratic approximation. We compare the B dependence for wells and T-shaped wires to show why the quadratic approximation is worse for T-shaped wires. Second, we determine the magnetic-field dependence of exciton energies in T-shaped wires.

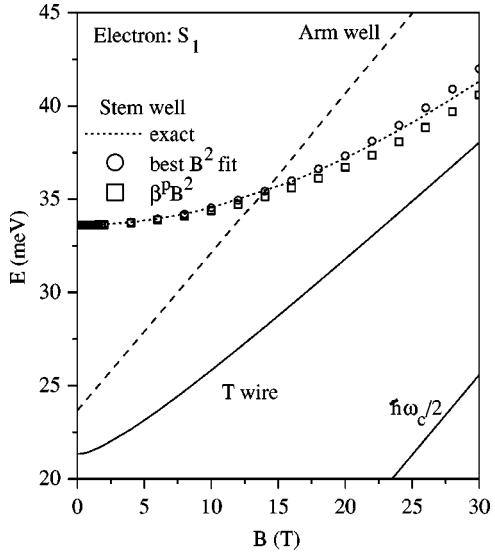

FIG. 2. Comparison of the field dependence for the electron energy in the T-shaped wire S_1, stem well of S_1, and arm well of S_1. B is applied perpendicular to the wire and parallel to the stem well. The stem-well width is 10 nm. The best quadratic fit and the exact quadratic contribution for an electron in the stem well are shown. The energy of a free, 3D electron is also shown.

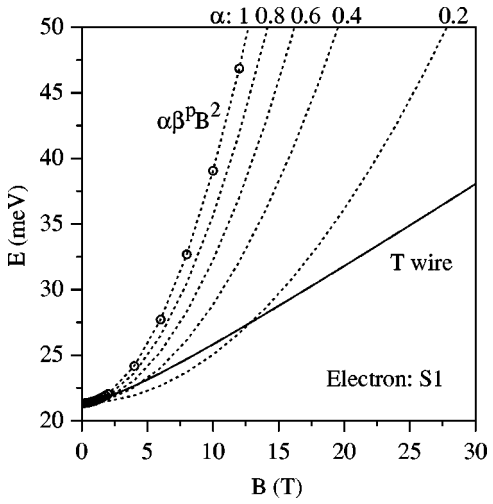

FIG. 3. Magnetic-field dependence of the electron energy in the T-shaped wire S_1. The field is applied perpendicular to the wire and parallel to the stem well. The exact energy is compared with the exact quadratic approximation. Other possible quadratic approximations are shown also.

A. Single particle states in a magnetic field

The exact field dependence for the energy of an electron confined in a quantum well (the 10 nm stem well in S_1) is shown in Fig. 2. B is applied parallel to the well. The exact electron energy is compared with the exact diamagnetic approximation [Eq. (14)] and a best quadratic fit to the exact calculation. From Fig. 2 we see that the exact quadratic approximation and the best quadratic fit, obtained for B from 0 to 30 T, are nearly identical and agree very well with the exact result. In this case, the B-field confinement is a weak perturbation of the quantum well confinement and the quadratic approximation is accurate to 30 T. For large B, the magnetic field confinement compresses the electron state, keeping the electron away from the well barriers. In this limit the effect of the well confinement becomes negligible. We see from Fig. 2 that the electron energy is well above the 3D cyclotron energy ($\hbar\omega_c/2$) even at 30 T. At 30 T, the cyclotron diameter is 6.6 nm, still just slightly less than the well width.

The exact ground-state energy for an electron in the S_1 T-shaped wire with B applied perpendicular to the wire axis and parallel to the stem well is shown in Fig. 3. For comparison, the exact quadratic approximation given by Eq. (14) and other possible quadratic approximations are shown. The quadratic approximation given by Eq. (10) for the symmetric gauge is undefined for a wire, just as it was undefined for a well. The exact quadratic approximation dramatically overestimates the field-dependent energy shift for almost the entire energy range of B that is shown. The exact quadratic approximation is accurate only for small fields ($B \lesssim 1$ T). Other quadratic approximations shown in Fig. 3 fail just as dramatically at large B and underestimate the exact energy at small B. The quadratic approximation is good only for small B and only if the exact diamagnetic contribution is used.

The magnetic-field dependence for the electron energy in a T-shaped wire (wire S_1), in the corresponding stem well, and in the corresponding arm well are compared in Fig. 2. The largest energy shifts occur for the arm well. The smallest energy shifts occur for the stem well. The field-dependence for the electron energy in the T-shaped wire exhibits a crossover between these two cases. For small B, the electron trapped at a T-shaped intersection is mostly in the arm well. When the field is increased, the electron is squeezed perpendicular to the field. This squeezing leads to an energy increase. In a T-shaped wire, the electron can leak into the stem well to compensate this energy increase. Thus the field-dependent single-particle energy-shift is weaker for a T-shaped wire than for an arm well. At large B, the single-particle energy for a T-shaped wire approaches the limit for the stem well.

Similar results apply for the other T-shaped wires. Figure 4 shows the field dependence for the electron energy in the smallest T-shaped wire, S_4. Confinement is stronger in S_4 than in the other wires and the quadratic approximation should be best for S_4. Even for S_4, the quadratic approximation fails for $B > 3$ T. The error in the field-dependent energy shift made by the exact quadratic approximation is small only for small fields ($B < 3$ T for S_4, $B < 0.5$ T for S_1). At 10 T, the error is nearly 50% for S_4 and nearly 300% for S_1. This comparison shows that the diamagnetic approximation, even if calculated exactly, should not be used to analyze energy shifts obtained for T-shaped wires at 10 T.

The weak field-dependence of the single-particle energy in T-shaped wires and the poor agreement between the quadratic approximation and the exact energy in T-shaped wires are due to the squishy confinement provided by a T-shaped wire. The lateral confinement and any energy increase induced by the applied field is compensated by leakage into the

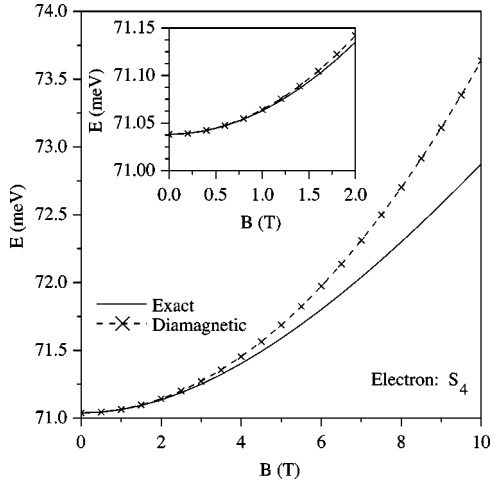

FIG. 4. Magnetic-field dependence of the electron energy in the T-shaped wire S_4. The field is applied perpendicular to the wire and parallel to the stem well. The exact energy is compared with the exact quadratic approximation. The agreement for small B is shown in the insert.

stem well and the resulting energy decrease. Figure 5 shows the size of the electron state along x and y as a function of B. The size is taken to be the root mean square of the electron position about the mean position of the electron. As B increases, the spread along x decreases monotonically for each wire, while the spread along y increases monotonically for each wire.

B. Magnetoexcitons

In this section, we show that the observed magnetic-field shifts for excitons trapped in T-shaped wires can be modeled when the single-particle energies are determined exactly and the Coulomb binding is included accurately. The quadratic approximation fails dramatically for single-particle energies

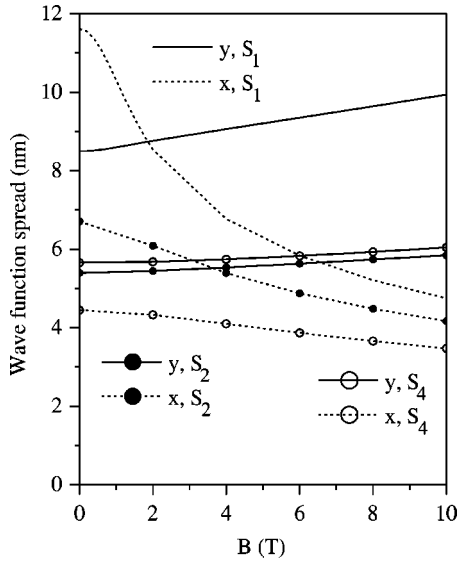

FIG. 5. Magnetic-field dependence of the electron ground-state width along x and y for T-shaped wires S_1, S_2, and S_4.

in T-shaped wires, even when the quadratic contribution is calculated exactly. In this section we also determine how accurately the quadratic approximation describes magnetoexciton energies in T-shaped wires.

The diamagnetic contribution given by β^L is the exact quadratic contribution for an exciton when the exciton is an eigenstate of L_y with $L_y=0$. However, an exciton trapped in a T-shaped wire is not an eigenstate of L_y. The diamagnetic contribution given by β^p is the exact quadratic contribution for an exciton when the exciton is an eigenstate of the electron and hole p_z with $p_z=0$. However, the exciton is not an eigenstate of the single-particle momenta. The second-order paramagnetic contribution is negative for the ground state, so the diamagnetic contribution overestimates the exact quadratic approximation for the exciton ground state. The smaller of β^L or β^p provides the more accurate diamagnetic approximation for the quadratic contribution. For thicker wires (S_1 and S_2), $\beta^L<\beta^p$ so β^L gives the better approximation. For thinner wires (S_3 and S_4), $\beta^p<\beta^L$ so β^p gives the better approximation. For wires made from wide wells, the Coulomb interaction should be dominant and the states should be approximate eigenstates of L_y. For wires made from thin wells, the single-particle confinement should be dominant and the exciton states should be approximate eigenstates of the single-particle p_z. The approximate symmetry of the exciton state determines which diamagnetic approximation is better.

The best diamagnetic approximation for the exciton energy shift, the exact single-particle energy shift for the electron-hole pair and the energy shift calculated for a 3D correlated exciton are shown in Figs. 6 and 7 for T-shaped wires S_1-S_4. Exciton energy shifts calculated for the isotropic-hole model are shown for S_1 and S_2. The anisotropic-hole model works better at zero field for S_3 and S_4. We show the exciton energy shifts calculated with the anisotropic-hole model for S_3 and S_4. The best diamagnetic approximation shown in each figure is given by the smaller of the two diamagnetic coefficients that are determined with the best zero-field model for the exciton. For S_1 and S_2, the best zero-field model has 3D correlation and an isotropic hole. For S_3 and S_4, the best zero-field model has 3D correlation and an anisotropic hole. For comparison, the diamagnetic approximation found including only the 1D correlation in the zero-field exciton state is shown. All results are plotted as energy shifts from the corresponding zero-field exciton energy. Also shown is the energy shift for the pair energy in the arm well, shifted upward for clarity by the single-particle trapping energy of the pair at the T intersection.

The results are similar for each wire. The diamagnetic contribution found from the model with only 1D correlation does not provide a reasonable description for the field-dependence of the exciton energy for any wire modeled. The diamagnetic contribution found from the model with 3D correlation is much smaller for each wire. This is another indication that correlation in all three dimensions must be included for a proper description of the exciton states. Even when the correlation is included accurately, the best diamagnetic contribution does not provide an adequate approximation for the exciton energy. The best diamagnetic approxima-

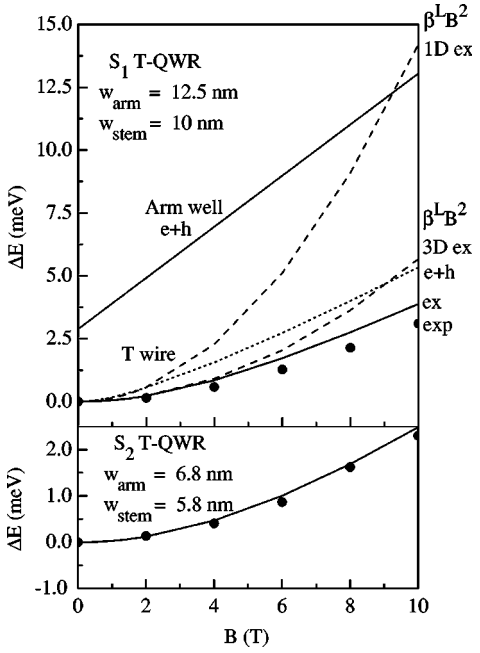

FIG. 6. The magnetic-field-induced energy shift for excitons trapped at S_1 and S_2 T-shaped wires: experimental shift[9] (solid circles), calculated shift for an uncorrelated pair in S_1 (dotted curve), calculated shift for a 3D-correlated exciton (lower solid curve), and the best approximation for the diamagnetic shift in S_1 (dashed curves, as indicated, for 3D- and 1D-correlated excitons). The best approximation for the diamagnetic shift for S_1 is given by β^L. For comparison, the electron-hole pair energy in the arm well is shown.

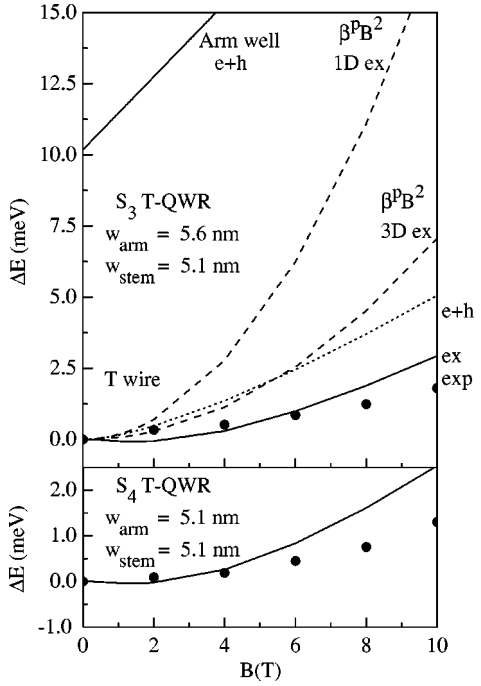

FIG. 7. The magnetic-field-induced energy shift for excitons trapped at S_3 and S_4 T-shaped wires: experimental shift[9] (points), calculated shifts for an uncorrelated pair in S_3 (dotted curve) and for a 3D-correlated exciton (lower solid curve), and the best approximation for the diamagnetic shift for S_3. The best approximation for the diamagnetic shift for S_3 is given by β^p. For comparison, the electron-hole pair energy in the arm well is shown. All calculations are done for the anisotropic hole model.

tion begins to deviate significantly from the experimental data for fields of 2–4 T and is a factor of 2 too big at 10 T. The data obtained at 10 T was used to determine empirically the exciton size. Our results show that such an analysis cannot be done above 2–4 T.

The experimental data can be modeled accurately provided that the exciton energy is calculated accurately at each *B*. The single-particle energies (the electron-hole pair energy shown in Figs. 6 and 7) and the pair binding must be determined accurately to obtain a good model for the field-dependence of the exciton energy shifts (curves labeled ex in Figs. 6 and 7). The single-particle energies overestimate the energy shift at low *B*. The single-particle energy shifts are too high at low fields because the wave function compression that is provided by pair-correlation is not included. At higher fields, the single-particle energies provide an energy shift that is lower than the energy shift obtained with the best diamagnetic approximation. The field dependence of the single-particle energies at high fields is weaker than the field dependence predicted by the diamagnetic approximation due to the squishy confinement. The effects of the squishy confinement are included when the single-particle energies are calculated exactly at each field. These effects are not included when the zero-field exciton state is used to determine the diamagnetic contribution in perturbation theory. When pair correlation is included and the exciton states are found accurately at each field, the exciton energy shift follows closely the experimental data. The pair correlation is needed to correctly model the weak field dependence at low fields. At high fields, the squishy confinement produces the weak response.

For large wires (S_1 and S_2), the isotropic hole model provides the best model for the exciton states at zero field. The isotropic model works well because the effects of hole subband splitting in large wires is weak, especially for exciton states made from strongly correlated electron-hole pairs. The *B* dependence for large wires obtained from the isotropic model agrees well with the experimental data. For smaller wires (S_3 and S_4), the anisotropic hole model provides a better model for the exciton states at zero field. The anisotropic model works better because it includes the effects of hole subband splitting that become important in smaller structures. The *B* dependence for S_3 and S_4 obtained with the anisotropic-hole model (shown in Fig. 7) is more accurate than the diamagnetic approximations. The isotropic-hole model for S_3 and S_4 provides a *B* dependence for the energy shifts (not shown in Fig. 7) that is even weaker than the shift obtained from the anisotropic model. The shifts obtained with isotropic model agree more closely with the data. At high fields, the squeezing provided by the field becomes important and the hole subband splitting provided by the structure becomes less important. Thus the isotropic model provides a better description at higher fields.

IV. CONCLUSION

Excitons in T-shaped wires typically are observed in photoluminescence. The energy shift between the PL peaks for wire and well excitons reveals the effect of the wire confinement on the electron and hole single-particle energies plus the enhancement of the binding due to confinement. Recently, exciton magnetophotoluminescence of T-shaped wires has been observed to provide additional complementary information about exciton states in T wires.[9,16,20] The field-induced exciton energy shifts observed for wires were smaller than the shifts for the corresponding quantum wells. This was taken to imply strong squeezing of the exciton by wire confinement. The measured field-induced energy shifts were analyzed assuming a quadratic field dependence determined by the diamagnetic energy. The small sizes extracted from the data for the wire excitons implied that the wire confinement was 1D quantum confinement. Our previous calculations for exciton states in wires at zero field[26] predict a much larger size for the exciton states that is inconsistent with the experimental analysis. To understand the magnetophotoluminescence experiments, we have done detailed calculations of the exciton states as a function of magnetic field. The single-particle states are calculated exactly at each field and used as the basis set for accurate calculations of the pair binding. We find that accurate calculations for the exciton states in T wires can explain the weak field-induced shifts that have been observed. A comparison of the accurate calculations and the energy shifts obtained from the diamagnetic contribution shows that the diamagnetic contribution drastically overestimates the energy shifts in T wires. The energy shifts cannot be analyzed based on a weak-field perturbation theory. If the T-wire confinement were 1D quantum confinement, then the magnetic-field-induced confinement could be treated as a weak perturbation. This is not the case in T-shaped wires. The T-wire confinement is weak, squishy confinement rather than 1D quantum confinement. This weak confinement is easily disrupted by a magnetic field. When a magnetic field is applied perpendicular to the arm well and the wire axis, the field squeezes the exciton state laterally in the arm well. Because the wire confinement is squishy, the squeezed exciton can leak out of the wire into the stem well along the field axis. The leakage out of the wire compensates any squeezing induced by the field and produces the small energy shifts observed experimentally.

ACKNOWLEDGMENT

This work was supported in part by the U.S.-Israel Binational Science Foundation.

*Electronic mail: garnett.bryant@nist.gov
†Electronic mail: band@bgumail.bgu.ac.il

[1] Y.-C. Chang, L.L. Chang, and L. Esaki, Appl. Phys. Lett. **47**, 1324 (1985).
[2] A.R. Goñi, L.N. Pfeiffer, K.W. West, A. Pinczuk, H.U. Baranger, and H.L. Stormer, Appl. Phys. Lett. **61**, 1956 (1992).
[3] W. Wegscheider, L. Pfeiffer, M.M. Dignam, A. Pinczuk, K.W. West, S.L. McCall, and R. Hull, Phys. Rev. Lett. **71**, 4071 (1993).
[4] R.D. Grober, T.D. Harris, J.K. Trautman, E. Betzig, W. Wegscheider, L. Pfeiffer, and K. West, Appl. Phys. Lett. **64**, 1421 (1994).
[5] W. Wegscheider, L. Pfeiffer, M. Dignam, A. Pinczuk, K. West, and R. Hull, Semicond. Sci. Technol. **9**, 1933 (1994).
[6] W. Wegscheider, L. Pfeiffer, K. West, and R.E. Leigenguth, Appl. Phys. Lett. **65**, 2510 (1994).
[7] J. Hasen, L.N. Pfeiffer, A. Pinczuk, H.U. Baranger, K.N. West, and B.S. Dennis, Superlattices Microstruct. **22**, 359 (1997).
[8] J. Hasen, L.N. Pfeiffer, A. Pinczuk, S. He, K.W. West, and B.S. Dennis, Nature (London) **390**, 54 (1997).
[9] T. Someya, H. Akiyama, and H. Sakaki, Phys. Rev. Lett. **74**, 3664 (1995).
[10] T. Someya, H. Akiyama, and H. Sakaki, Appl. Phys. Lett. **66**, 3672 (1995).
[11] T. Someya, H. Akiyama, and H. Sakaki, J. Appl. Phys. **79**, 2522 (1996).
[12] T. Someya, H. Akiyama, and H. Sakaki, Phys. Rev. Lett. **76**, 2965 (1996).
[13] H. Akiyama, T. Someya, and H. Sakaki, Phys. Rev. B **53**, R4229 (1996).
[14] H. Akiyama, T. Someya, and H. Sakaki, Phys. Rev. B **53**, R10520 (1996).
[15] H. Akiyama, T. Someya, and H. Sakaki, Phys. Rev. B **53**, R16 160 (1996).
[16] T. Someya, H. Akiyama, M. Yamauchi, H. Sugawara, and H. Sakaki, Solid-State Electron. **40**, 315 (1996).
[17] H. Akiyama, T. Someya, M. Yoshita, T. Sasaki, and H. Sakaki, Phys. Rev. B **57**, 3765 (1998).
[18] M. Yoshita, H. Akiyama, T. Someya, and H. Sakaki, J. Appl. Phys. **83**, 3777 (1998).
[19] H. Akiyama, J. Phys.: Condens. Matter **10**, 3095 (1998).
[20] T. Someya, H. Akiyama, and H. Sakaki, Solid State Commun. **108**, 923 (1998).
[21] W. Langbein, H. Gislason, and J.M. Hvam, Phys. Rev. B **54**, 14 595 (1996).
[22] H. Gislason, C.B. Sørensen, and J.M. Hvam, Appl. Phys. Lett. **69**, 800 (1996).
[23] H. Gislason, W. Langbein, and J.M. Hvam, Superlattices Microstruct. **20**, 1 (1996).
[24] H. Gislason, W. Langbein, and J.M. Hvam, Appl. Phys. Lett. **69**, 3248 (1996).
[25] W. Langbein, H. Gislason, and J.M. Hvam, Phys. Rev. B **60**, 16 667 (1999).
[26] G.W. Bryant, P.S. Julienne, and Y.B. Band, Superlattices Microstruct. **20**, 601 (1996).
[27] A.A. Kiselev and U. Rossler, Semicond. Sci. Technol. **11**, 203 (1996).
[28] F. Rossi, G. Goldoni, and E. Molinari, Phys. Rev. Lett. **78**, 3527 (1997).
[29] G. Goldoni, F. Rossi, E. Molinari, and A. Fasolino, Phys. Rev. B **55**, 7110 (1997).
[30] S. Glutsch, F. Bechstedt, W. Wegscheider, and G. Schedelbeck, Phys. Rev. B **56**, 4108 (1997).
[31] S.N. Walck, T.L. Reinecke, and P.A. Knipp, Phys. Rev. B **56**, 9235 (1997).

[32] D. Brinkmann and G. Fishman, Phys. Rev. B **56**, 15 211 (1997).
[33] M. Grundmann, O. Stier, A. Schliwa, and D. Bimberg, Phys. Rev. B **61**, 1744 (2000).
[34] G.W. Bryant, J.L. Bradshaw, R.P. Leavitt, M.S. Tobin, and J.T. Pham, Appl. Phys. Lett. **63**, 1357 (1993).
[35] Y. B. Band and G. W. Bryant, Bull. Am. Phys. Soc. **43**, 314 (1998); G. W. Bryant and Y. B. Band, *Proceedings of the 24th International Conference on the Physics of Semiconductors* (World Scientific, Singapore, 1999).
[36] S.N. Walck and T.L. Reinecke, Phys. Rev. B **57**, 9088 (1998).